Visualizing the Mott transition

Rajarshi Tiwari and Pinaki Majumdar*

Harish-Chandra Research Institute, Chhatnag Road, Jhusi, Allahabad 211 019, India

Correlated electronic systems involve strong short-range repulsion. At integer filling, the primary effect of correlation is the emergence of an insulating state where band theory predicts a metal. Understanding the transition from a metal to this 'Mott insulator', as interaction strength is increased, and the effect of doping the Mott state, are classic problems in quantum many-body physics. They have been explored for decades, starting with the approximate solutions of Hubbard. The real breakthrough came in the 1990s with the advent of dynamical mean field theory, which mapped the correlated system to an embedded single site, and described the detailed spectral evolution across the Mott transition. The only deficiency in this approach is the neglect of spatial correlations, and, possibly, the lack of some 'visual intuition' about the transition. We discuss a complementary approach, which provides a reasonable description of Mott physics in a real-space setting and allows a certain degree of visualization. This article provides a pedagogical review of our approach and presents some illustrative results.

Keywords: Correlated electron system, metal–insulator transition, magnetism.

Introduction

Correlated electron systems define a frontier in condensed matter and materials physics[1,2]. Experimentally, many of the fascinating discoveries of the last 25 years, e.g. high T_c superconductivity in the cuprates[3], 'colossal magnetoresistance' in the manganites[4], the high thermopower cobaltates[5], or the recently discovered pnictides[6] fall in this category. The theory of such materials is complicated because it involves strongly coupled quantum degrees of freedom and the tools of band theory or perturbation theory do not allow much headway. Interaction effects have to be handled non-perturbatively, and the standard numerical tools for such treatment, while providing benchmarks, have several limitations.

Although every class of material involves its own detail, condensed matter theorists often home in on some simple model that captures the essential physics, and build back the details later. Prominent among these is the Hubbard model[7,8] that describes the competition between electron delocalization (band-like character) and interaction-driven localization, i.e. a 'Mott insulator'[9]. It is worth defining the model right at the outset to set the notation and specify the parameter space.

$$H = \sum_{\langle ij\rangle\sigma} t_{ij} c^{\dagger}_{i\sigma} c_{j\sigma} - \mu \sum_i n_i + U \sum_i n_{i\uparrow} n_{i\downarrow}.$$

Qualitatively, it describes electrons moving on a lattice and incurring a cost when two electrons (with up and down spin) are present on the same site. $c^{\dagger}$ and c are electron 'creation' and 'annihilation' operators respectively. t_{ij} is the 'hopping' amplitude between sites located at $\mathbf{R}_i$ and $\mathbf{R}_j$. We will assume the simplest case of $t_{ij} = -t$ for nearest neighbour (*NN*) sites on a square lattice, and zero otherwise. n_i is the local electron density operator, and μ the chemical potential. $U > 0$ is the 'onsite' repulsion and penalizes the simultaneous presence of up- and down-spin electrons on the same site. We set $t = 1$.

The two parameters in the problem are electron density $n = N_{\rm el}/N_{\rm site}$ (where $N_{\rm el}$ is the number of electrons and $N_{\rm site}$ the number of lattice sites) and the ratio U/t. When $U/t \ll 1$, one expects the effect of interactions to be perturbative, unless there is something unusual about the susceptibilities of the non-interacting system. For $U/t \gg 1$ the system would try to avoid double occupancy, i.e. $n_{i\uparrow} n_{i\downarrow} \sim \mathcal{O}(1)$. This restricts the mobility as the density $n \to 1$, and promotes 'local moment' character in the electron system. At $n = 1$, one would obtain an electron localized phase, a 'Mott insulator', with vanishing d.c. conductivity and a gap in the electronic density of states. If we caricature the Mott insulator as essentially 'site localized' electrons, the arrangement of electron spins is decided by optimizing the kinetic energy from short-range excursion. Parallel arrangement, for example, is bad since the Pauli principle would prohibit the hopping of an up-spin electron to a neighbouring up-spin site. Thus, antiferromagnetism is generally preferred, and for the simple square lattice with *NN* hopping one obtains a Neel ordered state. The situation where $U/t \gg 1$ and $1 - n = x$ is small but finite is complicated, and is believed to be relevant to the physics of high-temperature superconductors[3].

We will specialize to $n = 1$ and the *NN* hopping model on a square lattice to focus on specific issues. We may want to know: (i) the nature of the ground state, metallic or insulating, and its magnetic character as U/t is varied; (ii) the effect of increasing temperature at fixed U/t, i.e. the thermal physics across the magnetic or insulator–metal transition and (iii) the effect of increasing U/t

*For correspondence. (e-mail: pinaki@hri.res.in)

remaining at some fixed finite temperature. In all these cases we would like to know measurable properties like magnetic structure, electronic density of states, resistivity, optical conductivity, etc.

A great deal is known about these issues for the model we have chosen, accumulated over the years from exact diagonalization (ED)[10], quantum Monte Carlo (QMC)[11] studies or via dynamical mean field theory (DMFT)[12,13]. The ED studies, unfortunately are severely size-limited (can access about size ~4 × 4) and are hard to push to finite temperature. QMC can access sizes ~10 × 10, but being an 'imaginary time' method, they do not yield spectral, transport or optical information readily. DMFT studies are by definition in the thermodynamic limit but lose information about spatial correlations. For the simple situation we discuss in this article, this can be remedied, but in lattices with geometric frustration, where complex magnetic order can arise, the limitation is real. Also, DMFT *implementations* often depend on ED or QMC and suffer the limitations described earlier[14].

A method for correlated systems should ideally handle large spatial scales accessing inhomogeneous structures, capture not only the ground state but also the thermal physics, provide information on spectral properties and provide some visual intuition about the physics. This is a tall order, and the exact numerical tools in standard use often fail to meet many of these requirements. We feel that a method that has the features above is worth exploring even if it is approximate. In what follows we discuss such an approach, essentially resurrecting ideas that go back four decades, to the work of John Hubbard[15], and implement it via modern numerical tools.

Formalism

For the Hubbard model, the Hilbert space grows too quickly with system size for exact diagonalization on any large system. One, therefore, has to resort to some method that recasts the problem as effectively 'non interacting'. Such a decomposition was provided by Stratonovich[16] and Hubbard[17]. The Hubbard–Stratonovich (HS) transformation maps the interacting electron problem to that of non-interacting electrons in a space–time fluctuating field. This is the starting point for many approximations[18].

We would like to use this HS transformation in a form where the rotation invariance of the original Hubbard model is retained. This was discussed by Hubbard[15], in his exploration of ferromagnetic order, and revisited by Schulz[19] in the context of antiferromagnetism. The interaction term in the functional integral that describes the system can be written as:

$$\exp[Un_{i\uparrow}n_{i\downarrow}] = \int \frac{\mathrm{d}\phi_i \mathrm{d}\vec{m}_i}{4\pi^2 U} \exp\left[i\phi_i n_i - \vec{m}_i \cdot \vec{\sigma}_i + \frac{\phi_i^2}{U} + \frac{\vec{m}_i^2}{U} \right].$$

n_i is the electron density, $\vec{\sigma}_i$ the electron spin operator, and ϕ_i and $\vec{m}_i$ are the scalar and vector auxiliary fields respectively. To recover the effect of the original Hubbard interaction one would have to solve the electron problem for all possible backgrounds $\{\phi_i(\tau), \vec{m}_i(\tau)\}$. The partition function:

$$Z = \int \mathcal{D}c\mathcal{D}\bar{c} \prod_i \frac{\mathrm{d}\phi_i \mathrm{d}\vec{m}_i}{4\pi^2 U} \exp\left[-\int_0^\beta \mathcal{L}(\tau) \right]$$

is now an integral over the Grassmann fields c and $\bar{c}$, and also the auxiliary fields $\vec{m}_i$ and ϕ_i.

$$\mathcal{L}(\tau) = \sum_{i\sigma} \bar{c}_{i\sigma} \partial_\tau c_{i\sigma} + H_0(\tau) + \sum_i [(i\phi_i - \mu) n_i - \vec{m}_i . \vec{\sigma}_i] + H_{\mathrm{cl}},$$

where $H_{\mathrm{cl}} = \sum_i (m_i^2 + \phi_i^2)/U$.

Full QMC calculations would retain the space–time dependence of the auxiliary fields on a small system, while DMFT would retain their dynamics at a single site. Our principal approximation is the neglect of dynamics for the auxiliary fields. We treat them as 'classical', i.e. static and time-independent[20]. This still allows the fields to fluctuate thermally at a given site at finite T, but suppresses the $T = 0$ *quantum fluctuations*. The static approximation has strengths and weaknesses that we discuss later. Further, we treat the scalar field ϕ_i at the saddle point level (i.e. ignore its thermal fluctuations). The saddle point value at half-filling exactly cancels the chemical potential ($\mu = U/2$).

With the overall static approximation and the saddle point ϕ_i, the effective Hamiltonian is given by

$$H_{\mathrm{eff}} = -t \sum_{\langle ij \rangle \sigma} c_{i\sigma}^\dagger c_{j\sigma} - \frac{U}{2} \sum_i \vec{m}_i \cdot \vec{\sigma}_i + \frac{U}{4} \sum_i \vec{m}_i^2 .$$

The approximation has mapped on the original Hubbard problem to electrons coupled to (auxiliary) magnetic moments $\vec{m}_i$. One sees the similarity to the 'double exchange model, or the classical Kondo lattice[21]. For a given $\vec{m}_i$ configuration, the electron problem is quadratic and the Hilbert space scales linearly with lattice size.

What decides the relevant $\{\vec{m}_i\}$ configurations? Neither the magnitude nor the orientation of $\vec{m}_i$ is a priori given. If H_{eff} is the Hamiltonian for the composite 'electron + $\vec{m}_i$' system, the Boltzmann weight for the $\vec{m}_i$s themselves can be obtained by tracing over the electrons. Formally:

$$P\{\vec{m}_i\} = \frac{1}{Z} Tr_{c,c^\dagger} \mathrm{e}^{-\beta H_{\mathrm{eff}}} .$$

$P\{\vec{m}_i\}$, unfortunately, is not analytically calculable when U/t is large.

To generate the 'equilibrium' configurations, governed by $P\{\vec{m}_i\}$, we use a real-space Monte Carlo (MC) technique. We start with a configuration of $\vec{m}_i$ with random magnitudes and orientation at high T. We then attempt an update $\vec{m}_i \to \vec{m}_i'$ at site $\mathbf{R}_i$. The energy

$$\mathcal{E} = -T \log Tr_{c,c^\dagger} e^{-\beta H_{\text{eff}}}$$

is computed before and after the attempted update, and $\Delta\mathcal{E} = \mathcal{E}\{\vec{m}_i\} - \mathcal{E}\{\vec{m}_i'\}$ is compared to $k_B T$ in the Metropolis spirit.

Since a single diagonalization costs $\mathcal{O}(N^3)$, a MC sweep over the lattice would cost $\sim N^4$, prohibitive for a large lattice. Algorithms have been developed to speed up the process. We make a cluster approximation for estimating the update cost[22]. $\Delta\mathcal{E}$ is calculated by diagonalizing a small cluster (of N_c sites, say) around the reference site (Figure 1), rather than the full lattice (of N sites). The MC was done for lattice of size $N = 24 \times 24$, with clusters of size $N_c = 8 \times 8$. The exact diagonalization of the clusters handles the effect of the large U accurately.

While the annealing is done based on the cluster algorithm, physical properties are computed over the whole lattice. We calculate the thermal average of the structure factor $S(\mathbf{q}) = \frac{1}{N^2}\sum_{ij}\langle \vec{m}_i \cdot \vec{m}_j \rangle e^{i\mathbf{q}\cdot(\mathbf{R}_i - \mathbf{R}_j)}$ at each temperature, which serves us as the order parameter of the magnetic transition. Using this we can locate the magnetic transition T_c. The electronic properties like density of states and transport are computed and averaged over equilibrium configurations of $\{\vec{m}_i\}$.

Results

Phase diagram

We illustrate the usefulness of this method in the much studied case of the two-dimensional square lattice Hubbard model[10–12]. We will comment on effects that arise in more complex 'frustrated' lattices at the end.

Figure 2 shows the U–T phase diagram of this model obtained via the Monte Carlo implementation of the auxiliary field scheme. It is well known that the ground state in this bipartite lattice is antiferromagnetically ordered at all U. The weak U ordering is driven by a divergent susceptibility $\chi_0(\mathbf{Q})$, at $\mathbf{Q} = \{\pi, \pi\}$, arising from the nested Fermi surface. This smoothly crosses over to the strong coupling ordered phase which is essentially a nearest neighbour Heisenberg antiferromagnet with Neel order, i.e. again at $\mathbf{Q} = \{\pi, \pi\}$ but with a larger moment. This answer can be derived from Hartree–Fock theory, and arises naturally as the temperature $T = 0$ limit of our scheme.

While the ground state can be readily captured by mean field theory (MFT), and MFT results agree qualitatively with QMC-based estimates, the transition temperature beyond weak coupling crucially involves the effect of fluctuations. At large U, the auxiliary moments remain more or less fixed in magnitude as T increases, but they have angular fluctuations controlled by a scale $J \sim t^2/U$. MFT misses this scale, whereas our implementation retains it, enabling us to capture the correct T_{corr} in Figure 2.

The identification of metallic or insulating regimes in the phase diagram is based on our study of the resistivity,

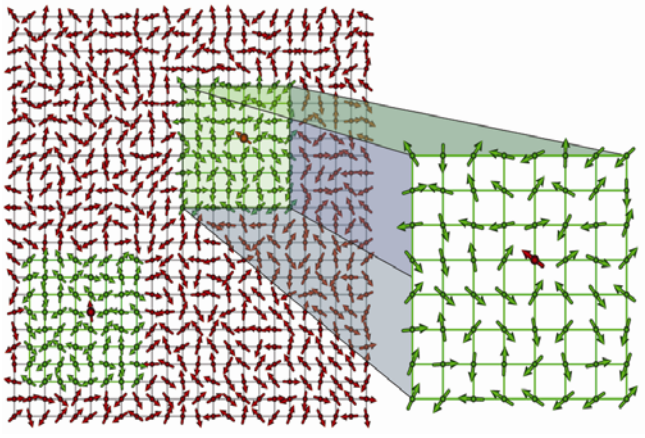

Figure 1. Schematic of the cluster-based Monte Carlo update. The 'spins' represent the auxiliary local moments $\vec{m}_i$. The electrons move in the background defined by these variables, and each update, in principle, requires diagonalization of the entire electronic Hamiltonian. If we are updating the moment at the centre of the top right green square, we diagonalize the electron Hamiltonian *only on the green cluster*. Similarly, for any other update site (bottom left, say). This dramatically reduces the computational cost, and makes the overall cost $\mathcal{O}(N)$, rather than $\mathcal{O}(N^4)$, where N is the system size.

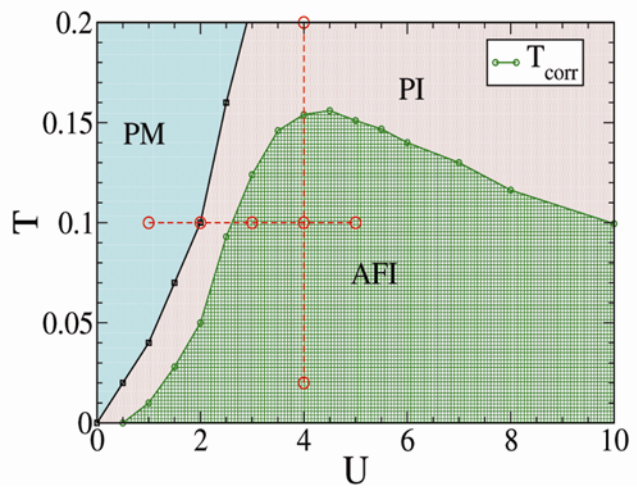

Figure 2. Phase diagram of the square lattice Hubbard model, with nearest neighbour hopping, at half-filling. There is no genuine magnetic transition in two dimensions, so we indicate the boundary between the paramagnetic phase and the antiferromagnet (AF) as a 'correlation temperature' T_{corr}, where the correlation length becomes comparable to system size. The AF phase is always insulating while the paramagnetic phase could be metallic or insulating. The two dotted lines indicate cross-sections that we discuss in detail in the text.

$\rho(T)$, shown in Figure 3. The resistivity shows insulating character at low T, in the antiferromagnetic (AF) phase, for all U, but a crossover to metallic behaviour at higher T when $U \lesssim 2.5$. There is a small window of paramagnetic insulating behaviour at small U, but this window widens rapidly with increasing U, and for $U \gtrsim 3$ there is no paramagnetic (PM) phase.

The thermal transition

Let us focus on $U = 4$, where $T_{corr} \sim 0.15$, to highlight how temperature affects physical properties. We examine the $\vec{m}_i$ distribution first, since this field dictates electronic properties. At low temperature $m_i = |\vec{m}_i|$ is essentially the same at all sites, whereas the orientation alternates. The distribution $P(m) = \langle \sum_i \delta(m - m_i) \rangle$ at low T should be sharply peaked. The angular brackets denote thermal average. Figure 4 bears this out at $T = 0.02$. At higher $T \sim 0.10$, still in the ordered phase, the mean value of m_i has increased but the distribution is also much broader. A single valued m_i with rigid AF correlation would of course have led to a more insulating state, but the high degree of amplitude fluctuation and loss of orientational correlation (Figure 5 below) actually weakens the insulating state. $P(m)$ at $T = 0.20$ has an even greater mean, but the broadening too is larger. Overall, in this intermediate U situation, increasing T tends to increase the typical magnitude of $\vec{m}_i$, but there is a rapid growth of amplitude fluctuations. What about angular fluctuations with increasing T?

Figure 5 shows snapshots of the 'classical background' that the electrons encounter. The top row shows typical maps of m_i at $T = 0.02$, 0.10, 0.20 (left to right). Remember these are individual thermal configurations, and control electronic properties. The second row shows the angular correlation map for the $\vec{m}_i$ configuration. We plot the overlap $\alpha_i = \vec{m}_0 \cdot \vec{m}_i$, where $\vec{m}_0$ is a fixed reference spin. The bottom row shows the magnetic structure factor $S(\mathbf{q})$ associated with the $\vec{m}_i$ configuration. This is meant to highlight the wavevector at which the moments correlate.

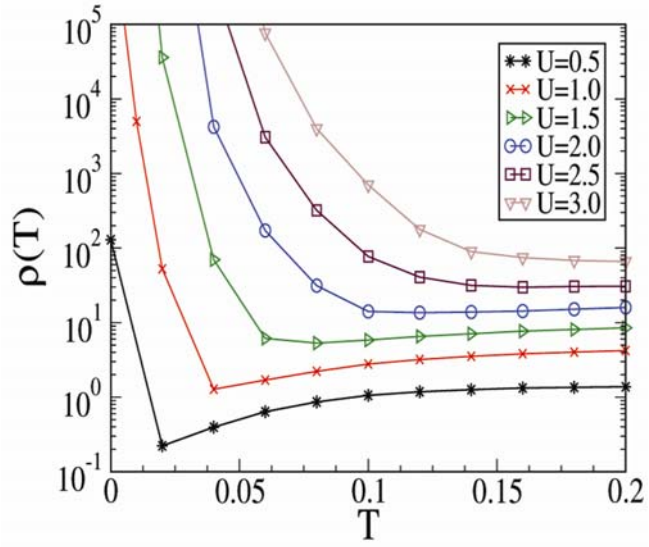

Figure 3. Temperature dependence of resistivity at different U. This 'd.c. resistivity' has a low temperature upturn at all U, indicating an insulating ground state. At low U, the resistivity has a crossover from insulating ($d\rho/dT < 0$) to metallic ($d\rho/dT > 0$) behaviour with increasing T. This occurs at a temperature slightly higher than T_{corr}, see Figure 2. For $U \gtrsim 2.5$, however, there is no 'metallic state' at moderate T.

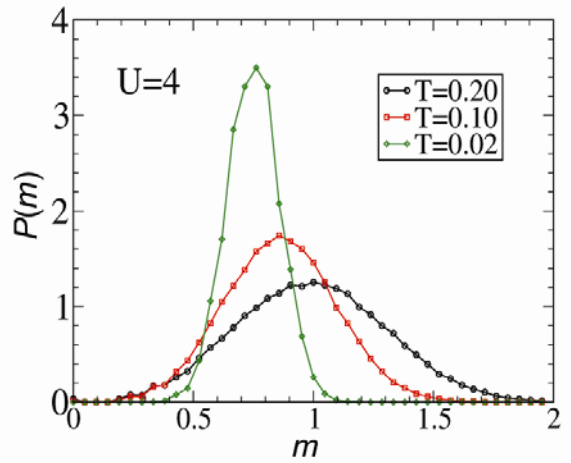

Figure 4. The distribution $P(m)$ of the magnitude of the auxiliary moment $\vec{m}_i$ averaged over sites and over Monte Carlo configurations at three different temperatures. The distribution should ideally be a delta function as $T \to 0$. It broadens progressively, and the mean value also increases as T increases.

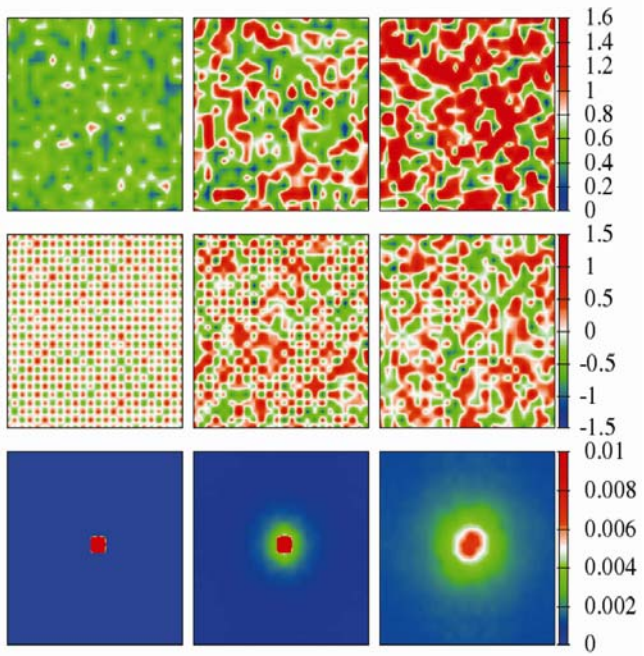

Figure 5. Snapshots of the auxiliary field and its correlations. Top row: $m_i = |\vec{m}_i|$; middle row: $\alpha_i = \vec{m}_0 \cdot \vec{m}_i$, where $\vec{m}_0$ is a fixed reference spin; bottom row: $S(\mathbf{q}) = N^{-2} \sum_{ij} \vec{m}_i . \vec{m}_j \exp(i\vec{q} \cdot (\mathbf{R}_i - \mathbf{R}_j))$. The spatial maps are on a 24 × 24 lattice, $S(\mathbf{q})$ is plotted between 0 and 2π on each axis. Temperatures along the row are $T = 0.02$, 0.10, 0.20.

At low T, the m_i snapshot is more or less homogeneous, with a mean value ~0.7. The associated α_i map shows alternating (Neel) pattern and $S(\mathbf{q})$ has a strong peak at $\{\pi, \pi\}$. This is roughly the MF ground state. For the middle column, $T = 0.10$, about $0.7T_{\text{corr}}$. The m_i mean is larger as $P(m)$ had indicated, but there is significant spatial fluctuation in m_i and the angular correlations show a domain pattern. On the right column, $T = 0.20 \sim 1.3T_{\text{corr}}$, the magnitude and angular fluctuations are even stronger and 'long-range order' is lost. There is still a diffuse scattering peak in $S(\vec{q})$ arising from short-range correlations.

Figure 6 shows the impact of thermal fluctuations on the density of states (DOS). The low T result shows the clean gap and sharp gap edge features expected from a Neel ordered background. With increasing T we see a narrowing of the gap and at $T = 0.20$ there is only a pseudogap in the spectrum. This transfer of spectral weight to low energies is driven by the increasing disorder in the $\vec{m}_i$ background, but the gap does not close due to the relatively large value of mean m_i. We have not shown the resistivity at $U = 4$ since it is too large for the scales in Figure 3, but it shows a monotonic fall with increasing T.

Interaction-driven Mott transition

The thermal transition that we discussed was related to the loss of magnetic order, the electronic properties continued to be insulating throughout. Also, since the ground state is always insulating, we cannot probe a metal–insulator transition (MIT) there with increasing U. However, at finite temperature there exists a PM phase, and we wish to understand the effect of increasing correlations starting with this finite T metal.

Figure 7 shows the evolution of the background fields as U increases at $T = 0.10$. We wish to probe the change in physical properties across the horizontal line in Figure 2, going from the paramagnetic metal to the AF correlated insulator. We have done a similar scan at $T = 0.20$ which goes from a paramagnetic metal to the paramagnetic (Mott) insulator, but cannot discuss that here due to space constraints. The principal observation in Figure 7 is the *increase in the typical value of m_i and decrease in the site-to-site fluctuation* as U increases. In parallel, the angular correlations become more prominent with increase in U, evolving from a short-range correlation at $U = 2$ to a progressively better AF ordered state for $U \geq 3$. The correlation length 'diverges' between $U = 2$ and $U = 3$. Figure 8 shows the $P(m)$ at $T = 0.10$ as U is increased. It clearly bears out the trend in the spatial plots about the mean and variance of m_i. What is the impact of this changing background on electronic properties?

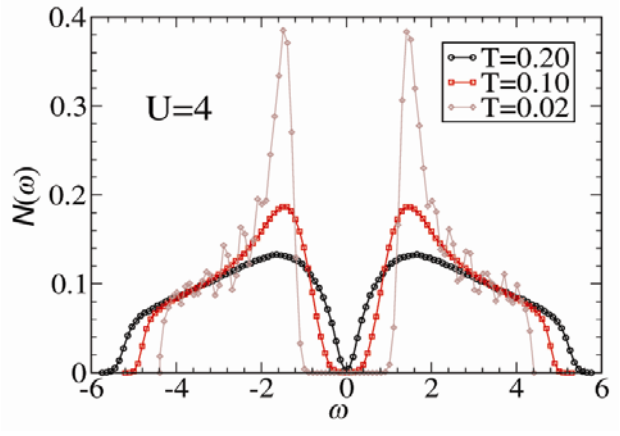

Figure 6. Density of states at $U = 4$, showing the thermal evolution. Note that although the mean m_i increases with T, the low T gap gradually closes with increasing T due to the strong disorder in $\vec{m}_i$.

Figure 9 shows the density of states and optical conductivity as U is increased. First the density of states. In response to the increase in the typical value of m_i, there is progressive transfer of spectral weight away from the Fermi level ($\omega = 0$) to the wings. $U = 2$ shows a weak pseudogap, $U = 3$ a much stronger dip (with vanishing DOS at ε_F), while $U = 4$, 5 has a clear gap in the spectrum. $U = 3$ onwards one can speak of the presence of Hubbard bands in the system.

The optics similarly shows a Drude feature at $U = 1$ and gapped character for $U \gtrsim 3$, but the most interesting result is for $U = 2$. Here the $\omega = 0$ conductivity is finite, so the system is a metal, but $\sigma(\omega)$ has a peak at finite frequency. The low value at $\omega = 0$ arises from the depleted DOS (top panel), and the finite frequency peak is crudely correlated with the separation between the two peaks in the DOS data. This bump in $\sigma(\omega)$ evolves into the 'inter Hubbard band' transition at large U.

Discussion

Within the static approximation our numerical method is quite accurate. The static approximation itself is quite effective in capturing most physical effects for the half-filled square lattice case that we have considered. So, in this particular case the corrections arising from the dynamics of $\vec{m}_i$ would be mostly quantitative. However, there are situations, notably magnetically frustrated lattices[23], and of course deviation from half-filling, where quantum fluctuations of $\vec{m}_i$ would be crucial. In what follows we mainly discuss the issues at half-filling on frustrated lattices.

There are broadly two shortcomings: (a) the poor description of a magnetically unordered metal, and (b) the description of geometrically frustrated insulators.

First (a). On structures which frustrate antiferromagnetic order, for example, the triangular or FCC lattice, the static method yields a ground state with $m_i = 0$ for $U < U_c$, where U_c depends on the lattice type. This is poor on two counts. (i) For $U < U_c$, it completely misses the 'high energy' effects associated with U, e.g. the formation of Hubbard satellites, and just yields the tight

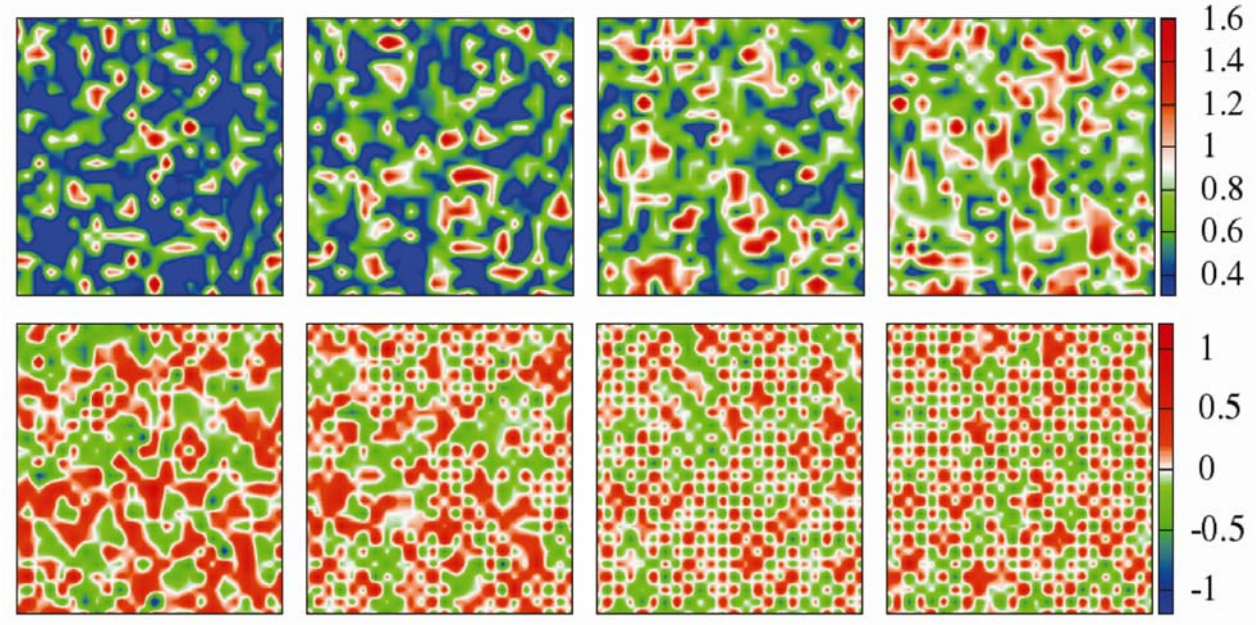

Figure 7. Snapshot of the $\vec{m}_i$ configuration at $T = 0.10$ for $U = 2, 2, 3, 5$. Top: auxiliary moment magnitude m_i. Bottom: the angular correlation α_i (see text). The electrons see these as typical configurations as the system evolves from a correlated metal to an antiferromagnetic insulator.

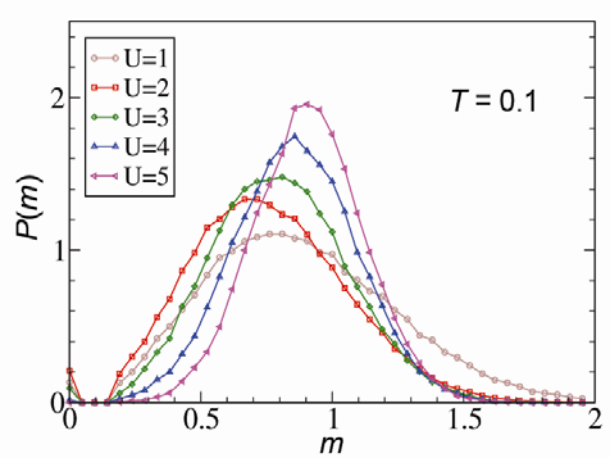

Figure 8. The $P(m)$ distribution, showing an increase in the mean, and progressive narrowing as U is increased.

binding result. (ii) It misses the renormalization of the low-energy physics (Fermi liquid corrections like enhancement of effective mass, etc.) arising from Kondo like physics.

For (b), magnetism in geometrically frustrated insulators, the method yields the ground state of a classical model of the form $J_{ij}\vec{m}_i \cdot \vec{m}_j$, where J_{ij} is a short-range interaction. On a triangular lattice, for example, this would generate a 120° phase, while the full quantum calculation suggests a spin liquid. The role of quantum fluctuations in destroying magnetic order in frustrated $S = 1/2$ systems is not captured by this approach.

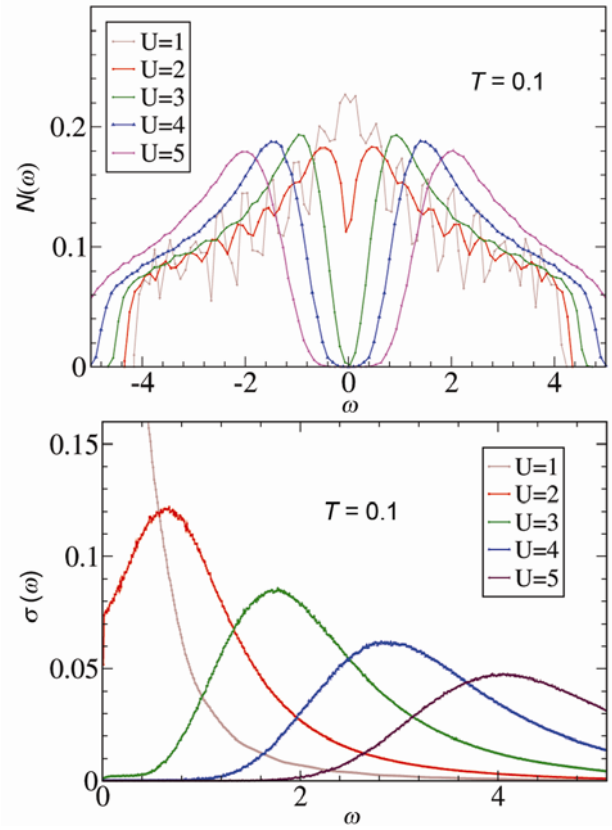

Figure 9. Indicators for the metal–insulator transition as U varies from 1 to 5 at $T = 0.10$. Top: the density of states, showing the evolution from an essentially tight binding DOS at $U = 1$ to the gapped state at $U = 5$, through a pseudogap regime. Bottom: the optical conductivity $\sigma(\omega)$, showing the evolution from a Drude response at $U = 1$ to a 'bad metal' response at $U = 2$, and then a gapped feature for $U \gtrsim 3$.

Conclusion

We have discussed a real-space approach to correlated electron systems, illustrating it in the case of metal–insulator transition in the two-dimensional Hubbard model. The approach, we feel, is intuitive, reproduces most benchmarks, and is tractable with computational resources available today. Generalization to more complex phases and models is the subject of ongoing research.

1. For a recent collection of articles, see Ong, N. P. and Bhatt, R. N. (eds), *More is Different: Fifty Years of Condensed Matter Physics*, Princeton University Press, 2001.
2. Dagotto, E., Complexity in strongly correlated electronic systems. *Science*, 2005, **309**, 257–262.
3. Lee, P. A., Nagaosa, N. and Wen, X. G., Doping a Mott insulator: Physics of high-temperature superconductivity. *Rev. Mod. Phys*., 2006, **78**, 17–85.
4. Tokura, Y. (ed.), *Colossal Magnetoresistive Oxides*, CRC Press, 2000.
5. Lee, M. *et al*., Large enhancement of the thermopower in Na_xCoO_2 at high Na doping. *Nature Mater*., 2006, **5**, 537–540.
6. Abrahams, E. and Si, Q., Quantum criticality in the iron pnictides and chalcogenides. *J. Phys.: Condens. Mat.*, 2011, **23**, 223201.
7. Hubbard, J., Electron correlations in narrow energy bands. *Proc. R. Soc*., 1963, **276**, 238–257.
8. Gutzwiller, M. C., Effect of correlation on the ferromagnetism of transition metals. *Phys. Rev. Lett*., 1963, **10**, 159–162.
9. Gebhard, F., *The Mott Metal–Insulator Transition: Models and Methods*, Springer, 2010.
10. Dagotto, E., Moreo, A., Ortolani, F., Poilblanc, D. and Riera, J., Static and dynamical properties of doped Hubbard clusters. *Phys. Rev. B*, 1992, **45**, 10741–10760.
11. Moreo, A., Scalapino, D. J., Sugar, R. L., White, S. R. and Bickers, N. E., Numerical study of the two-dimensional Hubbard model for various band fillings. *Phys. Rev. B*, 1990, **41**, 2313–2320.
12. Georges, A., Dynamical mean-field theory of strongly correlated fermion systems and the limit of infinite dimensions. *Rev. Mod. Phys*., 1996, **68**, 13–125.
13. Kotliar, G., Savrasov, S. Y., Haule, K., Oudovenko, V. S., Parcollet, O. and Marianetti, C. A., Electronic structure calculations with dynamical mean-field theory. *Rev. Mod. Phys*., 2006, **78**, 865–951.
14. Jarrell, M., Hubbard model in infinite dimensions: A quantum Monte Carlo study. *Phys. Rev. Lett*., 1992, **69**, 168–171; Caffarel, M. and Krauth, W., Exact diagonalization approach to correlated fermions in infinite dimensions: Mott transition and superconductivity. *Phys. Rev. Lett.*, 1994, **72**, 1545–1548.
15. Hubbard, J., The magnetism of iron. *Phys. Rev. B*, 1979, **19**, 2626–2636.
16. Stratonovich, R. L., On a method of calculating quantum distribution functions. *Sov. Phys. Dokl.*, 1958, **2**, 416.
17. Hubbard, J., Calculation of partition functions. *Phys. Rev. Lett*., 1959, **3**, 77–78.
18. Weng, Z. Y., Ting, C. S. and Lee, T. K., Path-integral approach to the Hubbard model. *Phys. Rev. B*, 1991, **43**, 3790–3793.
19. Schulz, H. J., Effective action for strongly correlated fermions from functional integrals. *Phys. Rev. Lett*., 1990, **65**, 2462–2465.
20. Similar ideas were discussed in Ramakrishnan, T. V., The Mott transition. *Curr. Sci*., 1990, **59**, 1125–1134.
21. Pradhan, K. and Majumdar, P., Magnetic order beyond RKKY in the classical Kondo lattice. *Eur. Phys. Lett*., 2009, **85**, 37007(1-6).
22. Kumar, S. and Majumdar, P., A travelling cluster approximation for lattice fermions strongly coupled to classical degrees of freedom. *Eur. Phys. J. B*, 2006, **50**, 571–579.
23. For a typical example, see Sahebsara, P. and Senechal, D., Hubbard model on the triangular lattice: spiral order and spin liquid. *Phys. Rev. Lett*., 2008, **100**, 136402(1-4).

ACKNOWLEDGEMENTS. We acknowledge use of the HPC clusters at the Harish-Chandra Research Institute, Allahabad. P.M. acknowledges support from the DST India (Athena), a DAE–SRC Outstanding Research Investigator grant, and discussions with T. V. Ramakrishnan.